Load–Displacement Relations of a Driven Steel Pipe Piles from Static and Rapid Load Tests, and Empirical Formulas Based on SPT and CPT: A Case Study at Sashima Test Yard

Shihchun Lin, Koji Watanabe, Yutaro Naka, and Tatsunori Matsumoto

Abstract Empirical formulas for estimating the shaft resistance τ_f and the tip resistance q_b of a vertically loaded pile are widely used all over the world. Standard penetration test (SPT) N-value or cone penetration test (CPT) tip resistance q_t is used in the empirical formulas. Coefficients used in the empirical formulas have been determined through the comparison with static load test (SLT) results. In this study, SLTs and rapid load tests (RLTs) were carried out on driven steel pipe piles (SPPs) at the test site of Jibanshikenjo Co., where SPT and CPTs were densely conducted. The shaft resistance and the tip resistance measured in SLTs are compared with those from RLTs as well as various pile design formulas. Furthermore, load–displacement relations from SLTs are compared with those τ_f, q_b, and shear moduli of surrounding soils estimated using empirical formulas.

Keywords Load–displacement relation · Bearing capacity · Steel pipe pile · Static load test · Rapid load test · Design codes

S. Lin (✉) · Y. Naka
Jibanshiknjo Co. Ltd., Tokyo, Japan
e-mail: s_rin@mail.jibanshikenjo.co.jp

Y. Naka
e-mail: y_naka@mail.jibanshikenjo.co.jp

K. Watanabe
Aichi Institute of Technology, Nagoya, Japan
e-mail: k-watanabe_28@aitech.ac.jp

T. Matsumoto
Kanazawa University, Kanazawa, Japan

P. Duc Long and N. T. Dung (eds.), *Proceedings of the 5th International Conference on Geotechnics for Sustainable Infrastructure Development*, Lecture Notes in Civil Engineering 395, https://doi.org/10.1007/978-981-99-9722-0_16

1 Introduction

Jibanshikenjo Co. Ltd. carried out comparative tests of static load test (SLT) and rapid load tests (RLTs) on driven steel pipe piles (SPPs) at the Sashima test yard, Ibaraki Prefecture, Japan. Standard penetration test (SPT) and electric cone penetration tests (CPTs) were carried out prior to the comparative tests [1].

In this study, the shaft resistance τ_f and the tip resistance q_b measured in SLTs are compared with those from RLTs as well as various pile design formulas. Furthermore, load–displacement relations from SLTs are compared with those from RLTs and also with those τ_f, q_b, and shear moduli of surrounding soils estimated using empirical formulas.

This paper discusses the reliabilities and advantages of RLTs and empirical methods.

2 Pile Load Test

2.1 Site Conditions

Figure 1 shows the results of soil investigations (SPT N-value, cone resistance corrected for pore pressure at filter q_t) and embedment of the instrumented test piles.

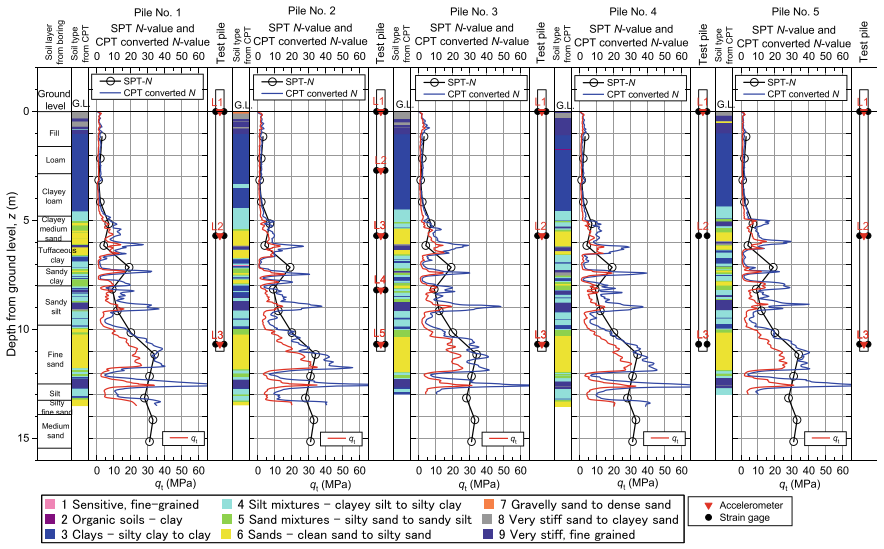

Fig. 1 Profiles of soil layers, SPT N-values and CPT q_t, together with instrumented test piles

Table 1 Specifications of test piles

Item	Value	
	Original	With protection
Pile length, L (m)	11.8	
Embedment length, L_d (m)	11.0	
Outer diameter, D_o (mm)	318.5	
Inner diameter, D_i (mm)	305.3	
Wall thickness, t_w (mm)	6.6	
Cross-sectional area, A (m^2)	0.00651	0.00926
Circumferential length, U (m)	1.00	1.20
Young's modulus, E (GPa)	205	
Density, ρ (ton/m^3)	7.81	
Bar wave velocity, c (m/s)	5123	
Mass, m (ton)	0.610	0.819

2.2 Test Piles

Table 1 shows the specifications of the test steel pipe piles (SPPs). Channel steels were welded on the test SPPs for protecting strain gages and accelerometers.

Pile No. 4 was instrumented with strain gages at three levels as shown in Fig. 1. Accelerometers were set at the only top level (L1).

2.3 Results of Pile Load Test [2]

In Pile No. 4, RLTs were carried out eight days after the step loading SLT. In RLTs, a hammer mass $m_h = 3.5$ ton was used and eight blows (RLTs) were applied to the pile with increasing drop height h from 0.03 to 0.83 m. The ultimate stage was reached at the eighth blow.

Figure 2 shows the pile head load–displacement relations and the pile tip load–displacement relations of Pile No. 4 from SLT and RLTs with ULPC_CM interpretation. In this study, q_b and τ_f from SLT and RLTs were estimated at the maximum loads, respectively.

3 Design Equations Specified in Various Codes

Tables 2 and 3 show the empirical equations for q_b and τ_f of driven piles, based on unified CPT design method for sand [3] and clay [4].

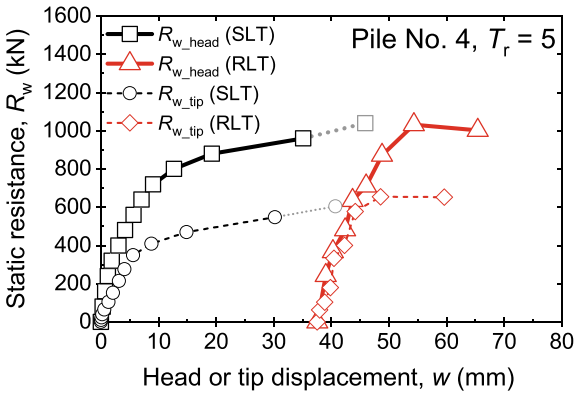

Fig. 2 Static load–displacement relations from SLT and RLTs (Pile No. 4)

Table 2 Estimation of maximum tip resistance q_b and maximum shaft resistance τ_f based on unified CPT method for sand

$q_b = 0.4q_c\left[\exp(-2 \times PLR) + 4t/D_o\right] \le 0.4q_c$
$\tau_f = 0.39(\sigma'_{rc} + \Delta\sigma'_{rd})$
$\sigma'_{rc} = (q_c/44)A_{re}^{0.3}\left[Max\left[1,\ h/D_o\right]\right]^{-0.4}$
$\Delta\sigma'_{rd} = (q_c/10)(q_c/\sigma'_v)^{-0.33}(d_{CPT}/D_o)$
$A_{re} = 1 - PLR(D_i/D_o)^2$
$PLR = \tanh\left[0.3(D_i/d_{CPT})^{0.5}\right]$; $d_{CPT} = 35.7$ mm
q_c = cone tip resistance, t = pile wall thickness, h = height of given point on shaft above the pile base, σ'_v = in situ vertical effective stress, d_{CPT} = diameter of cone

Table 3 Estimation of maximum tip resistance q_b and maximum shaft resistance τ_f based on unified CPT method for clay

$q_b = (0.2 + 0.6A_{re})q_t$
$\tau_f = 0.07F_{st}\,q_t\ \mathrm{Max}\left[1, (h/D^*)\right]^{-0.25}$
$D^* = \left(D_o^2 - D_i^2\right)^{0.5}$ for an open -ended pile
$F_{st} = 1$ for organic clay, silty clay to clay, clayey silt to silty clay
$F_{st} = 0.5 \pm 0.2$ for sensitive, fine-grained clays
q_t = cone resistance corrected for pore pressure at filter

Table 4 shows the empirical equations for q_b and τ_f of driven piles specified in various Japanese codes.

4 Estimation Method of Load–Displacement Relation

For estimating load–displacement relation of a pile, shear moduli G of surrounding soils are necessary as described in Sect. 4.2.

4.1 Empirical Equations for Estimating Shear Modulus of Soil

Tables 5 and 6 show the empirical equations for estimating shear wave velocity V_s using SPT N-value and CPT data, respectively.

With the V_s estimated from Tables 5 and 6, shear modulus G_0 at small strain was estimated using Eq. (1) in this study:

$$G_0 = V_s^2 \rho \tag{1}$$

Here, ρ is the soil density.

4.2 Numerical Model of Pile–Soil System

Figure 3 shows the numerical model of pile–soil system. The responses of the whole pile subjected to static pile head load are calculated using a one-dimensional FEM. The pile is modeled as a series of linear elastic springs, and non-linear soil resistance behavior is considered at each pile node.

The soil resistance parameters in Fig. 4 are related to the soil properties as follows [11]:

Initial spring stiffness per unit area of the base resistance of the close-ended pile base:

$$k_{b0} = \frac{4\,G_0}{\pi\, r_o(1-v)} \tag{2}$$

Initial spring stiffness per unit area of the shaft resistance:

$$k_{s0} = \frac{G_0}{r_o}\frac{1}{\ln(r_m/r_o)} \tag{3}$$

Table 4 Estimation of maximum tip resistance q_b and maximum shaft resistance τ_f based on Japanese codes

Code	Tip/ Shaft (kPa)	Soil type		Note
		Sand	Clay	
Road [5]	Tip, q_b	$130N$ ($\leqq$ 6500)	$90N$ ($\leqq$4500)	
	Shaft, τ_f	$5N$ ($\leqq$ 100)	$6N$ or $1c$ ($\leqq$70)	c = cohesion (undrained shear strength)
Port [6]	Tip, q_b	300 ηN ($\leqq$ 15,000)	$6c$	$N = (N_1 + N_2)/2$, N_1 = N-value of the ground at pile tip, N_2 = mean N-value in $4D_o$ above the pile tip, η = plugging efficiency
	Shaft, τ_f	$2N$ ($\leqq$100)	$1c$ ($\leqq$100)	
Archi [7]	Tip, q_b	$300\eta N$ ($\leqq$18,000)	$6c$ ($\leqq$18,000)	$\eta = 0.16\left(L_B / D_i\right)$ for $2 \leq \left(L_B / D_i\right) \leq 5$ η=0.8 for $5 < \left(L_B / D_i\right)$ L_B = embedment length into bearing stratum, D_i = inner pile diameter
	Shaft, τ_f	$2N$ ($\leqq$100)	$0.8c$ ($\leqq$100)	
Railway [8]	Tip, q_b	$210N$($\leqq$10,000)	6.3c or $75N$ ($\leqq$20,000)	for CPP, N = mean N-value in the $3D_o$ below the pile tip
		$175N$ ($\leqq$8000)	$55N$ or $5.5c$ ($\leqq$16,000)	for OPP w/ $D_o \leqq 0.8$ m and $l/D_o > 5$, N = N-value of the ground at the pile tip, l = equivalent embedment length into bearing stratum, $l = [5\ D_o\ (N_1 + N_2)/2]/N$, N_1 = N-value at $5D_o$ above the pile tip, N_2 = N-value of the ground at pile tip, D_o = outer pile diameter
		$35(l/D_o)N$ ($\leqq$8000)	$11(l/D_o)N$ or $1.1(l/D_o)c$ ($\leqq$16,000)	for OPP w/ $D_o \leqq 0.8$ m and $l/D_o \leqq 5$, N = N-value of the ground at the pile tip
		$(140/D_o)N$ ($\leqq$8000)	$(44/D_o)N$ or $(4.4/D_o)c$ ($\leqq$16,000)	for OPP w/ $D_o > 0.8$ m and $l/D_o > 5$, N = N-value of the ground at the pile tip
		$(28/D_o)(l/D_o)N$ ($\leqq$8000)	$(8.8/D_o)(l/D_o)N$ or $(0.88/D_o)(l/D_o)c$ ($\leqq$ 16,000)	for OPP w/ $D_o > 0.8$ m and $l/D_o \leqq 5$, N = N-value of the ground at the pile tip
	Shaft, τ_f	$3N + 30$ ($\leqq$150)	$6N$ or $0.4c$ ($\leqq$120)	for CPP
		$3N$ ($\leqq$120)	$6N$ or $0.4c$ ($\leqq$120)	for OPP

CPP Close-ended pipe pile, *OPP* Open-ended pipe pile

Table 5 Estimation of shear wave velocity from SPT N-value (Diluvium) [9]

Clay	$V_s = 130N^{0.29}$ (m/s)
Sand	$V_s = 110N^{0.30}$ (m/s)
Gravel	$V_s = 140N^{0.26}$ (m/s)

Table 6 Estimation of shear wave velocity using CPT data [10]

$Q_{t1} = (q_t - \sigma_{vo})/\sigma'_{vo}$
$F_r = [f_s/(q_t - \sigma_{vo})]100\%$
$I_c = [(3.47 - \log Q_{t1})^2 + (\log F_r + 1.22)^2]^{0.5}$
$\alpha_{vs} = 10^{(0.55Ic+1.68)}$ (m/s^2)
$V_s = [\alpha_{vs}(q_t - \sigma_{vo})/p_a]^{0.5}$ (m/s)
q_t = corrected cone resistance f_s = sleeve friction σ_{vo} = in situ total vertical stress σ'_{vo} = in situ effective vertical stress p_a = atmospheric pressure ≈ 100 kPa

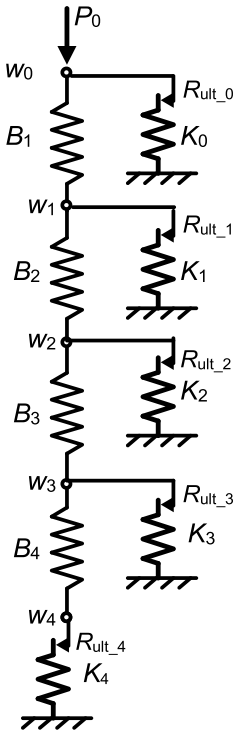

Fig. 3 Numerical model of pile–soil system

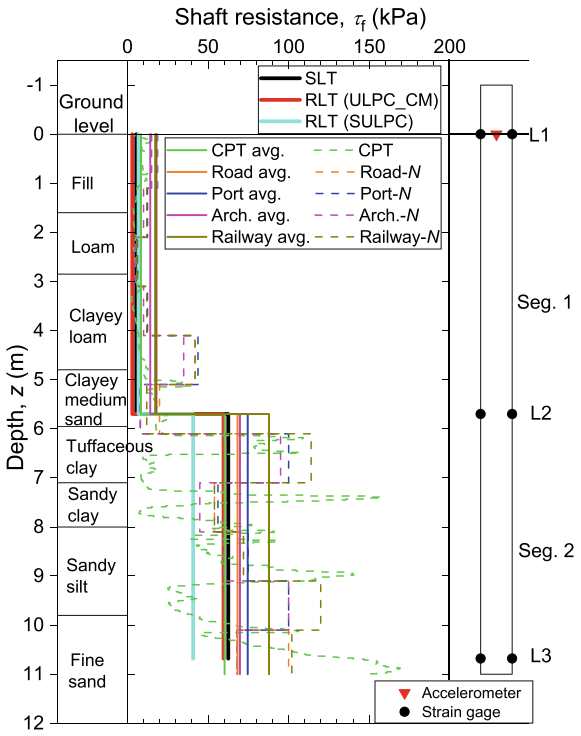

Fig. 4 Distributions of shaft resistance τ_f from SLT, RLT, and design codes (Pile No. 4)

Influential radius:

$$r_m = 2.5L(1 - \nu) \tag{4}$$

Here, r_o is pile outer radius, ν is Poisson's ratio of soil, and L is embedment length of the pile.

To express the non-linear soil resistance behavior, the spring stiffnesses were updated in the calculation process by Eqs. (5) and (6) according to [12].

$$k_b = k_{b0} \cdot \left(1 - R_{fb} \cdot \frac{q}{q_b}\right) \tag{5}$$

$$k_s = k_{s0} \cdot \left(1 - R_{fs} \cdot \frac{\tau}{\tau_f}\right) \tag{6}$$

Here, R_{fb} and R_{fs} are reduction factors for k_b and k_s, respectively. And, q and τ are mobilized base resistance and shaft resistance, respectively.

Soil spring stiffness is integrated respect to shaft area of each pile element, or respect to pile base area.

5 Comparison of Pile Resistances and Load–Displacement Relations from SLT with Those from RLT and Various Codes

Figure 4 shows the distributions with depth of shaft resistance τ_f from the SLT, RLT with ULPC_CM and SULPC interpretations [2], and various design codes.

Notice that when the empirical equation using only c is specified in the Japanese codes, $c = 6.25N$ (kPa) was assumed. F_{st} was set as 0.3 in the unified CPT method (Table 3).

In Fig. 4, the dotted lines are the shaft resistanceτ_f estimated from the various design codes. The solid lines indicate the average values of τ_f along the pile segment 1 (Seg. 1) and Seg. 2. The thick solid lines are the measured τ_f in SLT and RLTs.

To estimate the soil resistance on each pile segment, ULPC_CM interpretation analysis was carried out using the measured signals at each measurement level (L1, L2, and L3). When the signals measured at L1 are used, the soil resistance below L1 is obtained. Similarly, when the signals measured at L2 are used, the soil resistance below L2 is obtained. When signals measured at L3 are interpreted, the soil resistance is the pile tip resistance. Hence, the soil resistance acting on each segment was obtained.

Figure 5 shows the comparison of shaft resistance τ_f of two pile segments from SLT, RLT, and the design codes. Although there is no big difference between Japanese codes, Japanese codes overestimate the SLT result. On the other hand, the shaft resistance τ_f from CPT and RLT are almost equal to the SLT result.

Figure 6 shows the comparison of maximum total shaft resistance Q_s and maximum total tip resistance Q_b from SLT, RLT, and the design codes. The trend of Q_s is similar to that described in Fig. 5. There is a wide variation in Q_b from the design codes including the CPT method. The plugging efficiency $\eta = 1$ in Port code

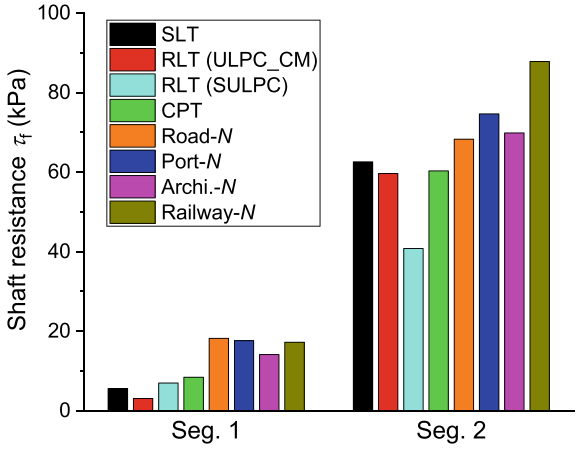

Fig. 5 Comparison of average shaft resistance τ_f of two pile segments from SLT, RLT, and design codes (Pile No. 4)

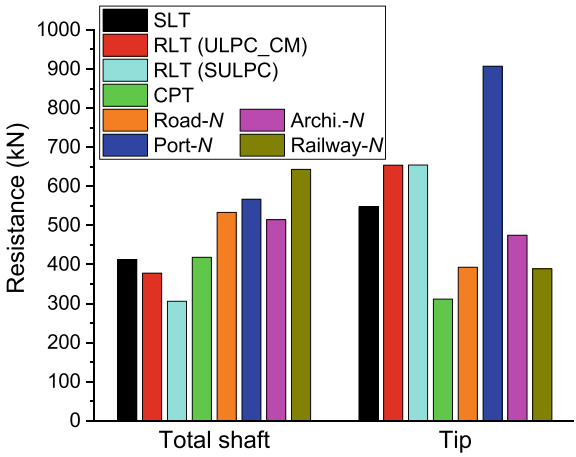

Fig. 6 Comparison of maximum total shaft resistance Q_s and maximum total tip resistance Q_b from SLT, RLT, and design codes (Pile No. 4)

and Road code, while $\eta = 0.52$ in Architectural code for this particular test pile condition.

Q_b from RLT is the most reasonable estimation for the SLT result.

Figure 7 shows the comparison of axial force distributions at ultimate states from SLT, RLT with ULPC_CM interpretation and SULPC interpretation, and the design codes.

The axial force distributions from the design codes and RLT with ULPC_CM were obtained by stacking the maximum shaft resistance, starting from the maximum tip resistance Q_b. In case of CPT, the stacking interval is 0.02 m, while it is 1 m in SPT.

Changes in axial force from various design codes including the CPT method show similar trends. Since the *N*-value was used in Japanese design codes, the changes of the axial force occur at 1-m intervals, while the axial force from CPT method shows more detail axial force changing at 0.02-m intervals. Axial force distributions from RLT with ULPC_CM and SULPC interpretations correspond very well to the SLT result.

Figure 8 shows the comparison of load–displacement relations from SLT, RLT, and the design codes. Load–displacement relations from RLT with ULPC_CM and SULPC interpretations corresponds very well to the SLT result. Load–displacement relations from Road, Architecture, and Railway codes also correspond well to the SLT result. Note that reduction factors R_{fs} and R_{fb} (Eqs. 5 and 6) were assumed to be 0.9 in the one-dimensional FEM analyses.

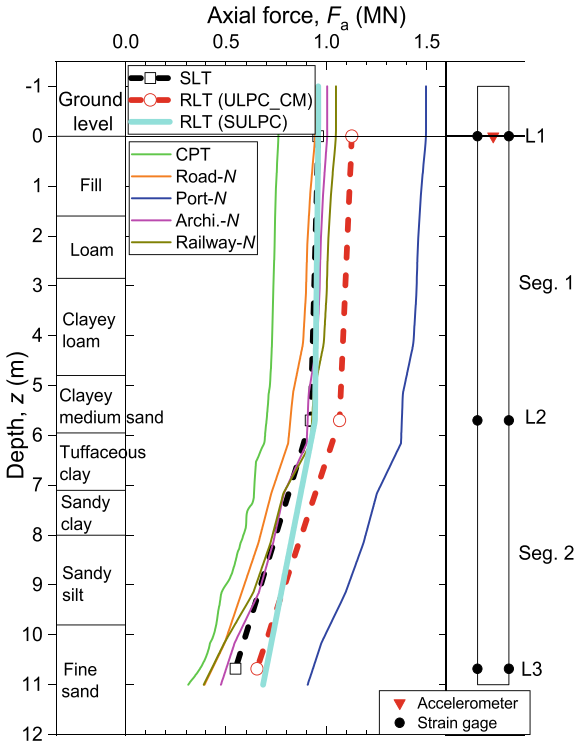

Fig. 7 Comparison of axial force distributions at ultimate states from SLT, RLT, and design codes (Pile No. 4)

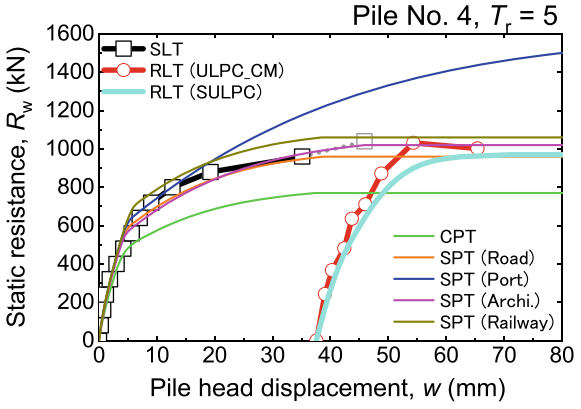

Fig. 8 Comparison of load–displacement relations from SLT, RLT, and design codes (Pile No. 4)

6 Conclusions

Comparative tests of SLT and RLT on a driven steel pipe pile were carried out in this study. SPT and CPTs were carried out prior to the comparative tests. The maximum tip resistance q_b and the maximum shaft resistance τ_f estimated from RLT and empirical formulas in various codes were compared with the results from SLT.

There was no significant difference in shaft resistance τ_f and tip resistance q_b between SLT, RLT with ULPC_CM, and RLT with SULPC in both test piles. On the other hand, there were large variations of τ_f and q_b from the various design codes. The results of RLT were the most comparable to the SLT results.

The load–displacement relation from RLT with ULPC_CM and SULPC was the most comparable to the SLT results in both test piles. The load–displacement relations from Road, Architecture, and Railway codes also correspond well to the SLT in both test piles.

Empirical equations may be used efficiently in preliminary design stage. However, it is strongly recommended to carry out RLTs in the final design stage.

Appendix 1: ULP Method

In the ULP interpretation method, the pile is assumed to be a rigid body having a mass m supported by a non-linear spring K and a linear dashpot as shown in Figure 9. The load on the pile F_{rapid} is resisted by the inertia of the pile R_a, velocity-dependent resistance R_v and the static soil resistance R_w (Eq. 7). The soil resistance R_{soil} is obtained from Eq. (8), using the measured F_{rapid} and α, and R_{soil} vs w is constructed as shown in Fig. 10. The static resistance R_w is then obtained using Eq. (9), if the damping constant C is determined. The R_{soil} at the maximum displacement point (ULP) is equal to the static resistance R_w because the pile velocity v is regarded as zero at ULP (Eq. 10 and Fig. 10).

When the Hybridnamic test is employed, generally five to seven blows are applied to the pile increasing the fall height of hammer h. Hence, several values of R_{ULP} at different displacements w are obtained without determining the value of C because

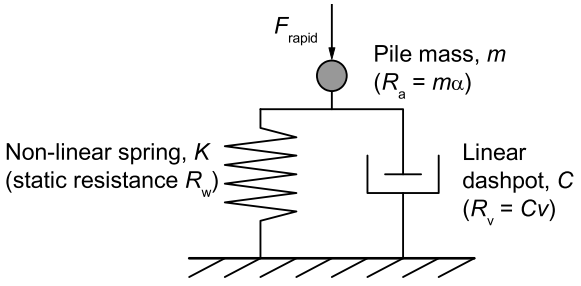

Fig. 9 Modeling of pile and soil during RLT (after Middendorp et al. 1993 [13], and Kusakabe and Matsumoto 1995 [14])

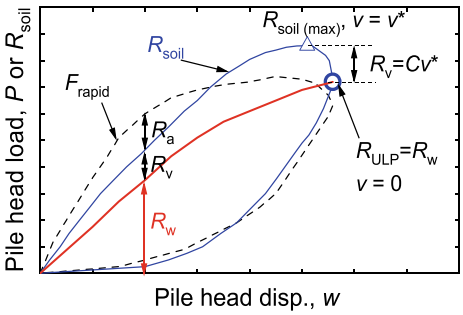

Fig. 10 Relationship between load–displacement curve and soil resistance and ULP resistance

the pile velocity v is zero at ULP, and R_w versus w ("static" load–displacement curve) is easily obtained by connecting ULPs. This method is named unloading point connection method (ULPC method).

This aspect is one of big advantages of the Hybridnamic test.

$$F_{\text{rapid}} = R_a + R_v + R_w = \text{ma} + Cv + R_w \tag{7}$$

$$R_{\text{soil}} = F_{\text{rapid}} - \text{ma} \tag{8}$$

$$R_w = R_{\text{soil}} - \text{Cv} \tag{9}$$

$$R_{\text{soil at ULP}} = R_{\text{ULP}} = R_w \tag{10}$$

Here, F_{rapid} = rapid load, R_a = inertial force of pile, R_v = dynamic resistance component of soil, R_w = static resistance component, m = pile mass, α = pile acceleration, C = damping constant, v = pile velocity, and R_{ULP} = ULP resistance (static resistance).

Appendix 2: ULPC Method

The ULPC method is an extension method of unloading point (ULP) method. In ULPC, the pile is treated as a single mass rigid body. To obtain soil resistance R_{soil}, the pile inertial force $R_a = m\,\alpha$(m = the pile mass and α = acceleration at pile head) is subtracted from the rapid load F_{rapid}. ULP is the point of R_{soil} at the maximum pile displacement w, where pile velocity $v = 0$. Hence, R_{soil} at ULP is equal to the static soil resistance R_w. By connecting ULPs from multiple blows, static load–displacement relation is easily obtained.

Table 7 Flow of SULPC

Step 1: Multicycle rapid load test
Step 2: Calculate relationship of soil resistance R_{soil}–displacement w and ULP load for each pile segment
Step 3: Construct static resistance R_w–displacement w relationship for each pile segment by connecting ULPs (SULPC)
Step 4: Analyze responses of elastic pile subjected to static loading using a load transfer method

Appendix 3: SULPC Method (Kamei et al. 2023 [15])

In the segmental unloading point connection (SULPC) method, forces and accelerations are measured at several sections of the pile.

As several blows are applied to the pile (step 1 in Table 7), static soil resistance of each segment is constructed by connecting ULPs (step 3).

The responses of the whole pile subjected to static pile head load are then calculated using a one-dimensional FEM (Fig. 3) (step 4). In this calculation stage, the pile is treated as elastic, and non-linear soil resistance behavior estimated in step 3 is considered at each pile node.

References

1. Lin S, Kamei S, Yamamoto I, Watanabe K, Matsumoto T (2023a) A case study on bearing capacities of driven steel pipe piles from load tests and empirical formulas based on SPT and CPT. In: Proceeding 2nd international conference of civil engineering—ICCE2023, Albania, pp 493–500
2. Lin S, Watanabe K, Kamei S, Yamamoto I, Matsumoto T (2023b) Comparative static and rapid load tests on steel pipe piles: A case study at Sashima test yard. In: Proceeding 5th international conference on geotechnics for sustainable infrastructure development, Hanoi (to be published)
3. Lehane B, Igoe D, Gavin K, Bittar E (2022a) Application of the Unified CPT method to assess the driving resistance of pipe piles in sand. In: Proceeding 11th international conference on stress wave theory and design and testing methods for deep foundations. The Netherlands. https://doi.org/10.5281/zenodo.7148654
4. Lehane BM, Liu Z, Bittar E, Nadim F, Lacasse S, Bozorgzadeh N, Jardine R, Ballard JC, Carotenuto P, Gavin K, Gilbert RB, Bergan-Haavik J, Jeanjean P, Morgan N (2022) CPT-based axial capacity design method for driven piles in clay. J Geotech Geoenv Eng 148(9):04022069
5. Japan Road Association (2017) Specification for Highway Bridges: Part IV Substructures
6. Ports and Harbours Bureau, Ministry of Land, Infrastructure, Transport and Tourism (MLIT) (2020) Technical Standards and Commentaries for Port and Harbour Facilities in Japan (abridged translation from The Overseas Coastal Area Development Institute of Japan https://ocdi.or.jp/en/)
7. Architectural Institute of Japan (2019) Guidelines for Building Foundation Structures (in Japanese)
8. Railway Technical Research Institute (2012) Design standards for railway structures and commentary: substructures (in Japanese)
9. Uchida A, Tokimatsu K, Tsujimoto K (2019) A consideration on shear wave velocity estimated by N-value. AIJ J Tech Des 25(59):119–122 (in Japanese)

10. Robertson PK (2009) Interpretation of cone penetration tests—a unified approach. Can Geotech J 46:1337–1355
11. Randolph MF, Deeks AJ (1992) Dynamic and static soil models for axial response. In: Proceeding 4th international conference application of stress wave theory to Piles. The Hague, A.A. Balkema Publishers, Brookfield VT, pp 3–14
12. Chow YK (1986) Analysis of vertically loaded pile groups. Int J Numer Analyt Methods Geomechan 10(1):59–72
13. Middendorp P, Bermingham P, Kuiper B (1992) Statnamic load testing of foundation pile. In: Proc. the 4th Intern. Conf. on Appl. of Stress-Wave Theory to Piles, The Hague:581–588
14. Kusakabe O, Matsumoto T (1995) Statnamic tests of Shonan test program with review of signal interpretation. In: Proc. the 1st Intern. Statnamic Seminar, Vancouver:13–122
15. Kamei S, Takano K, Fujita T (2022) Comparison of static load test and rapid load test on steel pipe piles in two sites. In: Proc. the 11th Int. Conf. on Stress Wave Theory and Design and Testing Methods for Deep Foundations, Rotterdam. https://doi.org/10.5281/zenodo.7148489